Supporting Information

Snyder et al. 10.1073/pnas.1215770110

SI Materials and Methods

Protein Expression and Purification. The human MyD88 (myeloid differentiation factor 88) cDNA encoding residues M157 to P296 was cloned into a pET30a-derived bacterial expression vector containing an N-terminal protein G β1 domain (GB1) tag followed by a tobacco etch virus (TEV) protease cleavage site. The GB1 coding plasmid was a gift from Gerhard Wagner at Harvard Medical School (Boston, MA). The TEV coding plasmid was a gift from Dr. David Waugh at the National Cancer Institute (Frederick, MD). The MyD88 construct was transformed into BL21 (DE3) Codon Plus RIPL cells (Stratagene). Cells were grown and induced with 0.5 mM Isopropyl β-D-1-thiogalactopyranoside (IPTG). Harvested cells were lysed in a buffer containing 25 mM Tris·HCl (pH 8.0), 300 mM NaCl, 10 mM imidazole, and EDTA-free protease inhibitor (Roche Applied Science). The soluble protein was purified using Ni-NTA beads (Qiagen). Further purification was carried out after TEV cleavage with a second immobilized metal ion affinity chromatography (IMAC) column and size exclusion chromatography. ^{15}N isotope labeled MyD88 Toll/IL-1 receptor (TIR) domain was expressed using $^{15}NH_4Cl$ (Cambridge Isotope Laboratories) as the sole nitrogen source in a minimal media (Molecular Dimensions) and purified as described above. Recombinant TcpC TIR domain (residues 170–307) was expressed using the pASK-IBA3-TIR-TcpC construct and purified as reported previously (1).

Crystallization and Structure Determination. Crystallization screening was carried out at 4 °C using the hanging drop method. The MyD88 TIR domain was crystallized in the presence of the TcpC TIR domain using a well solution containing 100 mM Tris·HCl (pH 8.0) and 25% (vol/vol) PEG 350 MME. Although TcpC was present in a 1:1 molar ratio with MyD88, no electron density for TcpC was observed in the crystal lattice. The MyD88 TIR domain was also lysine-methylated (2) and crystallized similarly in the absence of TcpC. Essentially the same structures were observed for both the native (1.45 Å resolution) and lysine-methylated (1.8 Å resolution) MyD88 TIR domains. Initial diffraction studies were carried out using the X-ray diffraction facility at National Institute of Diabetes and Digestive and Kidney Diseases, National Institutes of Health. Subsequent data collection was carried out at the Advanced Photon Source, Argonne National Laboratory (beam line Southeast Regional Collaborative Access Team 22 ID) and the National Synchrotron Light Source, Brookhaven National Laboratory (beam line X29). Data were processed with the HKL2000 program suite (3). The MyD88 crystal structure was solved by molecular replacement with the programs Amore and Phaser from the CCP4 Suite (4) using the deposited NMR structure of the MyD88 TIR domain (Protein Data Bank code 2JS7) as a search model. Model building was aided by Arp/Warp 7.0 (5) and carried out using the programs COOT (6) and O (7). Refinement was performed using the programs CNS (8) and PHENIX (9). The crystal structures were validated using Molprobity (10) in PHENIX and the Research Collaboratory for Structural Bioinformatics ADIT validation server (11). Solvent-accessible surface area was calculated with the program Areaimol from the CCP4 suite (4, 12). Figures were produced with Pymol (Schrödinger LLC).

Molecular Dynamics Simulation. The program suite GROMACS 4.5.5 (13) and CHARMM27 force field (14) were used for molecular dynamics (MD) simulations with the Biowulf Linux cluster at NIH. The MyD88 TIR domains were solvated with water molecules using the TIP3P water models (15). The structures were energy minimized using the steepest descent approach before subjecting to MD simulations for 5 or 10 ns with 2 fs steps at 300 K. The Particle-Mesh Ewald method for long-range electrostatics and the Linear Constraint Solver algorithm for covalent bond constraints were applied. Analysis of the MD simulation trajectories was carried out using the programs g_rms and g_rmsf in the GROMACS package. Separately computed 5-ns and 10-ns trajectories yielded very similar root mean square fluctuation profiles as in Fig. 2*B*.

Peptides. Peptides (Table S2) for the TcpC BB and DD loops were synthesized and HPLC purified by American Peptides, United Biosystems, or Thermo-Fisher Scientific. For the stimulation assays the peptides were synthesized as fusion with the TAT sequence. A short linker (AS) plus the Strep-tag II (WSHPQFEK) was added to the peptide sequences for the pull-down assays.

Pull-Down Assay. Purified TcpC TIR domain (TIR-TcpC) or the TcpC peptides carrying a C-terminal Strep-tag II were used as "bait." Eighty micrograms of purified TIR-TcpC or TcpC-loop peptides were bound to 50% (vol/vol) suspension of Strep-Tactin MacroPrep Beads (IBA) in buffer PD1 [100 mM Tris·HCl (pH 8.0), 1 mM EDTA, and 150 mM NaCl] for 1.5–3 h at 4 °C under gentle agitation. After three wash steps and one blocking step with avidin (300 μg/mL in PD1) at room temperature for 12 min under occasional rocking, 50–200 mg cleared total cell lysates ("prey") from HEK293 cells were added and incubated for 2 h at 4 °C followed by 30 min at 37 °C. The beads were then washed three times with an acetate buffer (product #1858605, Pierce/Thermo Scientific) containing 150 mM or 500 mM NaCl to remove nonspecifically bound proteins. The bound "prey" proteins were then eluted in two consecutive steps with an elution buffer (100 mM sodium citrate, 100 mM glycine, and 3 mM EDTA) at pH 2.8 and neutralized with 2 M Tris·HCl (pH 8.0). Samples were then stored at −20 °C before analysis by SDS/PAGE or Western blot.

To prepare the cell lysates, 5×10^6 HEK293 cells transfected using Lipofectamine 2000 (Invitrogen) with Myc-MyD88 or Flag-TLR4 (TLR, Toll-like receptor) plasmids were solubilized 24–48 h after transfection with a Nonidet P-40 lysis buffer containing 50 mM Hepes-Na (pH 7.6), 150 mM NaCl, 1 mM DTT, 1 mM EDTA, 1 mM EGTA, 0.5% (vol/vol) Nonident P-40, 0.125% (wt/vol) n-octyl-β-D-glucopyranoside, 10% (vol/vol) glycerol, 20 mM β-glycerolphosphate, 1 mM Na_3VO_4, 0.4 mM PMSF, and 1 mM NaF, plus the Complete protease inhibitor mixture (EDTA free, Roche Diagnostics). Lysates were subsequently dounced using a tissue grinder and dialyzed against PBS plus the protease inhibitor mixture.

Western Blot. All samples were reduced with the Lämmli buffer plus DTT and subjected to heat denaturation before SDS/PAGE. Myc-tagged MyD88 and Flag-tagged TLR4 were detected with Anti-Flag monoclonal antibody from Sigma-Aldrich and Anti-Myc antibody from Invitrogen diluted 1:1,000 in TBST buffer [100 mM Tris·HCl (pH 7.6), 150 mM NaCl, and 0.05% Tween-20). The secondary anti-mouse antibody (Jackson ImmunoResearch Europe) was diluted 1:5,000 in TBST, and the Western blot films were developed using standard procedures.

Cell Stimulation Assay. Bone marrow-derived macrophages (BMDMs) or J2 retrovirus-immortalized mouse BMDMs (kindly provided by Howard Young, National Cancer Institute, National Institutes of Health, Frederick, MD) were stimulated with the TLR ligands poly(I:C) (2.5 μg/mL), ultrapure LPS from *Escherichia coli*

(100 ng/mL), CpG-DNA 1826 (2 μM), or R848 (1 μM) in the absence or presence of titrated amounts of the TcpC peptides. Secreted TNF-α or keratinocyte chemoattractant (KC) was quantitated by ELISA from the culture supernatants 3 h after stimulation. All assays were performed in triplicate.

Mutagenesis of MyD88. Site-directed mutagenesis of MyD88 was performed with the plasmid pRK5-hMyD88-Myc using the following PCR-primer pairs: hMyD88-C203S forward (fw): 5′-CTGCCTGGCACCTCTGTCTGGTCTATTG-3′ and hMyD88-C203S reverse (rev): 5′- CAATAGACCAGACAGAGGTGC-CAGGCAG-3′; hMyD88-C280S fw: 5′- ACTACACCAACCC-CTCCACCAAATCTTG-3′ and hMyD88-C280S rev: 5′-CAA-GATTTGGTGGAGGGGTTGGTGTAGT-3′. The underlined bases indicate the mutation sites. After amplification, the parental methylated DNA templates were eliminated by enzymatic digestion with Dpn1 (NEB), and the remaining products were transformed in TOP10 competent cells (Invitrogen). Mutagenesis was confirmed by DNA sequencing (GATC Biotec).

Luciferase Reporter Assay. HEK293 cells were seeded in 96-well plates at a density of 3×10^4 cells per well in DMEM plus 10% FCS. The cells were transfected using Lipofectamine 2000 (Invitrogen) according to the manufacturer's instructions with NF-κB firefly luciferase (50 ng/mL) and Renilla luciferase reporter constructs (1 ng/mL), as well as plasmids encoding MyD88 wild type, C203S, C280S, or C203S plus C280S mutants. To test the inhibitory effects of TcpC, the TIR-TcpC ΔTAT plasmid at 0.2, 2, 20, or 200 ng/mL was cotransfected. The total amount of plasmid DNA was kept constant by transfection with empty vectors. At 48 h after transfection, cells were harvested, and the firefly luciferase activity was normalized to the activity of the Renilla luciferase. The luciferase activities were measured using the dual luciferase reporter assay system (Promega) and a microplate luminometer (Titertek Berthold). All assays were performed in triplicate.

NMR Titration of ^{15}N-labeled MyD88 TIR Domain with the TcpC TIR Domain. A 0.35-mM ^{15}N-labeled MyD88 TIR domain sample in PBS buffer (pH 6.5) was titrated with a 3-mM TcpC TIR domain stock solution to 1:1 molar ratio. The ^{1}H-^{15}N heteronuclear single quantum coherence spectra of MyD88 were recorded using a Brüker 800 MHz spectrometer, and the normalized ^{1}H-^{15}N chemical shift deviation (δ_{HN}) was calculated as $\sqrt{[\Delta H^2 + (\Delta N/5)^2]/2}$. The buffer effect was subtracted using another blank buffer titration. The mean value of the chemical shift difference is 4.2 ppb, and the SD is 2.1 ppb. The MyD88 residues with chemical shift changes of more than 7.3 ppb (mean + 1.5 SD) are M157, S244, K250, R269, F270, T272, V273, C280, and W286, which are presumably involved in interaction with TcpC. To examine the interaction of the TcpC DD loop with the MyD88 TIR domain, 0.01 mM of ^{15}N-labeled MyD88 TIR domain was mixed with a synthesized TcpC "DD-nostrand" peptide at 1:1 molar ratio. The MyD88-DD peptide complex sample was then concentrated to reach 0.1-mM protein concentration. The chemical shift changes were compared with a MyD88-only sample in the same buffer. The mean value of the chemical shift difference is 10.3 ppb and the SD is 8.79 ppb. The MyD88 residues with chemical shift changes of more than 23.5 ppb (mean + 1.5 SD) are V204, K250, L268, R269, C280, and W286, which are similar to those perturbed significantly by the TcpC TIR domain titration.

1. Cirl C, et al. (2008) Subversion of Toll-like receptor signaling by a unique family of bacterial Toll/interleukin-1 receptor domain-containing proteins. *Nat Med* 14(4): 399–406.
2. Walter TS, et al. (2006) Lysine methylation as a routine rescue strategy for protein crystallization. *Structure* 14(11):1617–1622.
3. Otwinowski Z, Minor W (1997) Processing of X-ray diffraction data. *Methods Enzymol* 276:307–326.
4. Potterton E, Briggs P, Turkenburg M, Dodson E (2003) A graphical user interface to the CCP4 program suite. *Acta Crystallogr D Biol Crystallogr* 59(Pt 7):1131–1137.
5. Perrakis A, Harkiolaki M, Wilson KS, Lamzin VS (2001) ARP/wARP and molecular replacement. *Acta Crystallogr D Biol Crystallogr* 57(Pt 10):1445–1450.
6. Emsley P, Cowtan K (2004) Coot: Model-building tools for molecular graphics. *Acta Crystallogr D Biol Crystallogr* 60(Pt 12 Pt 1):2126–2132.
7. Jones TA (2004) Interactive electron-density map interpretation: From INTER to O. *Acta Crystallogr D Biol Crystallogr* 60(Pt 12 Pt 1):2115–2125.
8. Brünger AT, et al. (1998) Crystallography & NMR system: A new software suite for macromolecular structure determination. *Acta Crystallogr D Biol Crystallogr* 54(Pt 5): 905–921.
9. Adams PD, et al. (2010) PHENIX: A comprehensive Python-based system for macromolecular structure solution. *Acta Crystallogr D Biol Crystallogr* 66(Pt 2): 213–221.
10. Chen VB, et al. (2010) MolProbity: All-atom structure validation for macromolecular crystallography. *Acta Crystallogr D Biol Crystallogr* 66(Pt 1):12–21.
11. Yang H, et al. (2004) Automated and accurate deposition of structures solved by X-ray diffraction to the Protein Data Bank. *Acta Crystallogr D Biol Crystallogr* 60(Pt 10): 1833–1839.
12. Lee B, Richards FM (1971) The interpretation of protein structures: Estimation of static accessibility. *J Mol Biol* 55(3):379–400.
13. Hess B, Kutzner C, van der Spoel D, Lindahl E (2008) GROMACS 4: Algorithms for highly efficient, load-balanced, and scalable molecular simulation. *J Chem Theory Comput* 4:435–447.
14. MacKerell AD, et al. (1998) All-atom empirical potential for molecular modeling and dynamics studies of proteins. *J Phys Chem B* 102(18):3586–3616.
15. Jorgensen WL, Chandrasekhar J, Madura JD, Impey RW, Klein ML (1983) Comparison of simple potential functions for simulating liquid water. *J Chem Phys* 79:926–935.

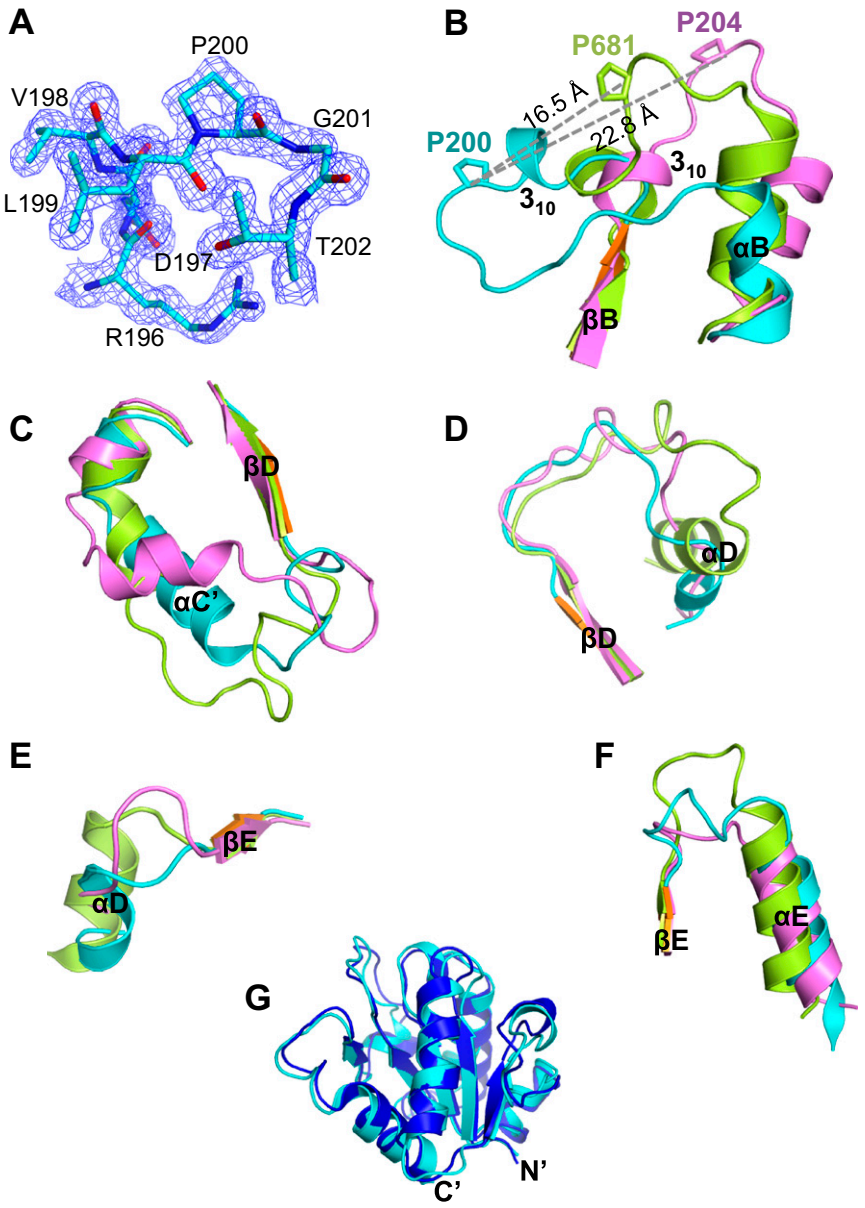

Fig. S1. Crystal structure of the MyD88 TIR domain. (*A*) 2Fo-Fc map (blue) calculated at 1.45-Å resolution and contoured at 1.2 sigma is shown for the MyD88 TIR domain BB loop. The significant structural differences among the MyD88 (cyan), TLR2 (green), and PdTLP (magenta) TIR domains are shown near the BB loop (*B*), CD loop (*C*), DD loop (*D*), DE loop (*E*), and EE loop (*F*). (*G*) Superposition of the crystal (cyan) and NMR (blue) structures of the MyD88 TIR domains. The orientation is the same as that in Fig. 1*A*.

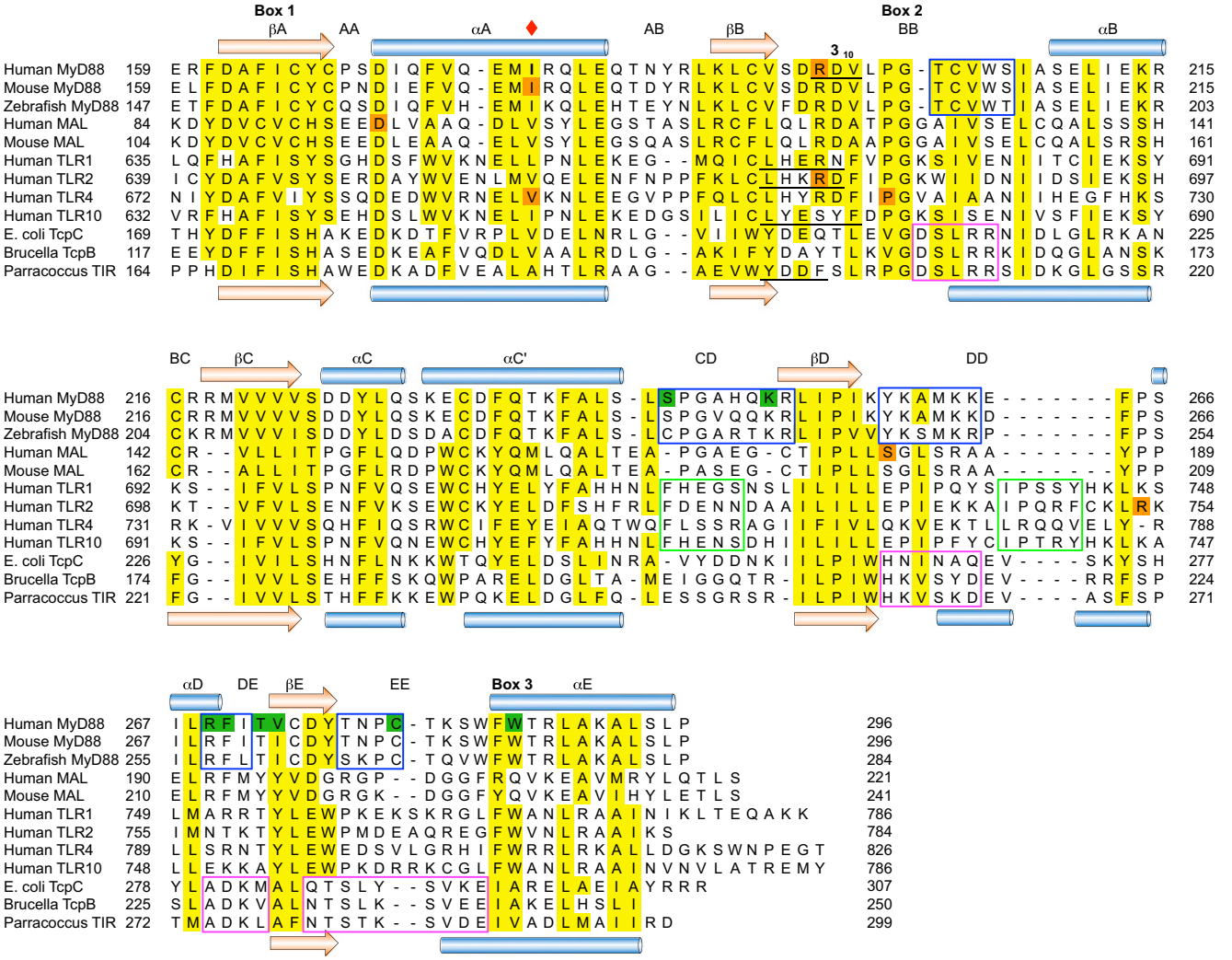

Fig. S2. Sequence alignment of selected TIR domains. Secondary structures of the MyD88 and *Paracoccus* PdTLP TIR domains are shown as arrows (β) and cylinders (α) above and below the sequences, respectively. The connecting loops and conserved boxes 1–3 are marked. The 3_{10} or α-helices within the BB loop regions of the known structures are underlined. The functionally important residues identified in human or mouse are shaded in orange, and residues perturbed by TcpC titration in green. The Poc site residue is also marked with a red diamond. The conserved residues among all TIR domains are shaded in yellow, those conserved among MyD88 TIR domains are in blue boxes, among the receptor TIR domains in green boxes, among the microbial TIR domains in magenta boxes.

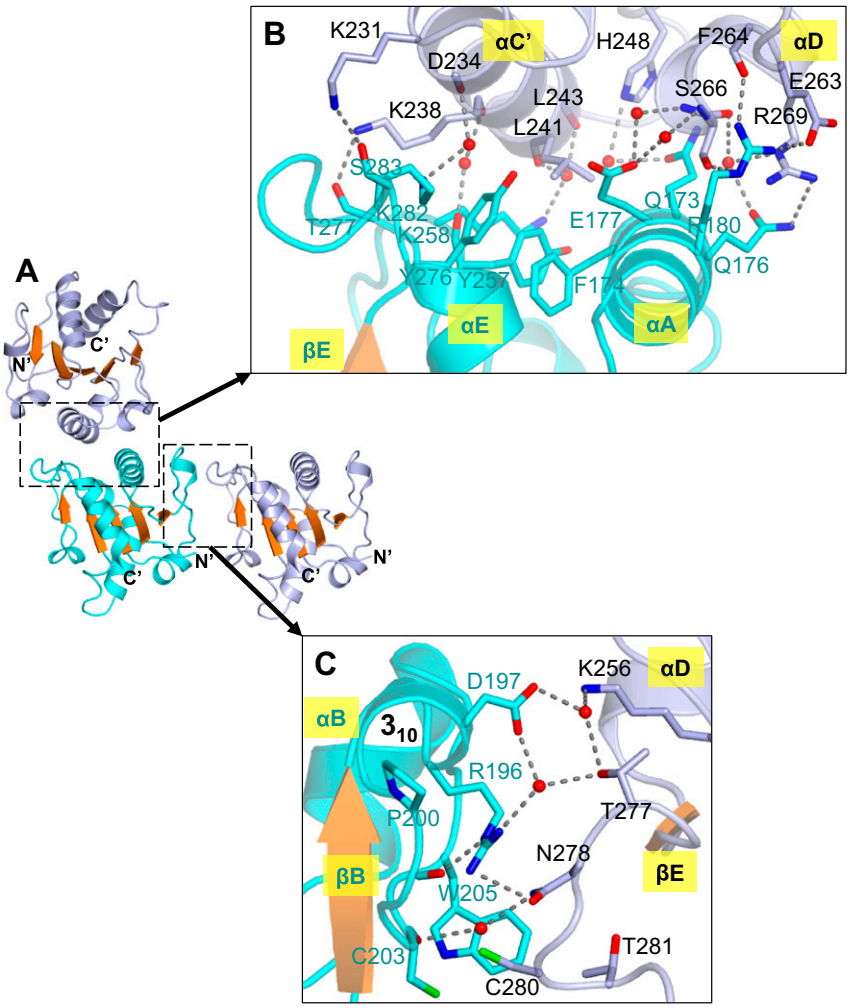

Fig. S3. MyD88 TIR domain crystal lattice interactions. (*A*) Overview of the two crystal lattice interfaces that bury significant amount of surface area. The unique TIR domain in the crystal is colored cyan, and its symmetry mates are colored light blue. The five β-strands are colored orange to show the relative orientations of the TIR domains. The detailed views of these interfaces are shown in *B* and *C*, with the hydrogen bonds indicated as gray dotted lines and water molecules as red spheres.

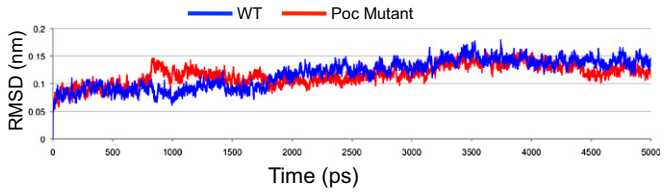

Fig. S4. The rmsd of the wild-type (blue) and I179N mutant (red) MyD88 TIR domains are shown as a function of the simulation time, suggesting that the systems reached equilibrium states for both proteins.

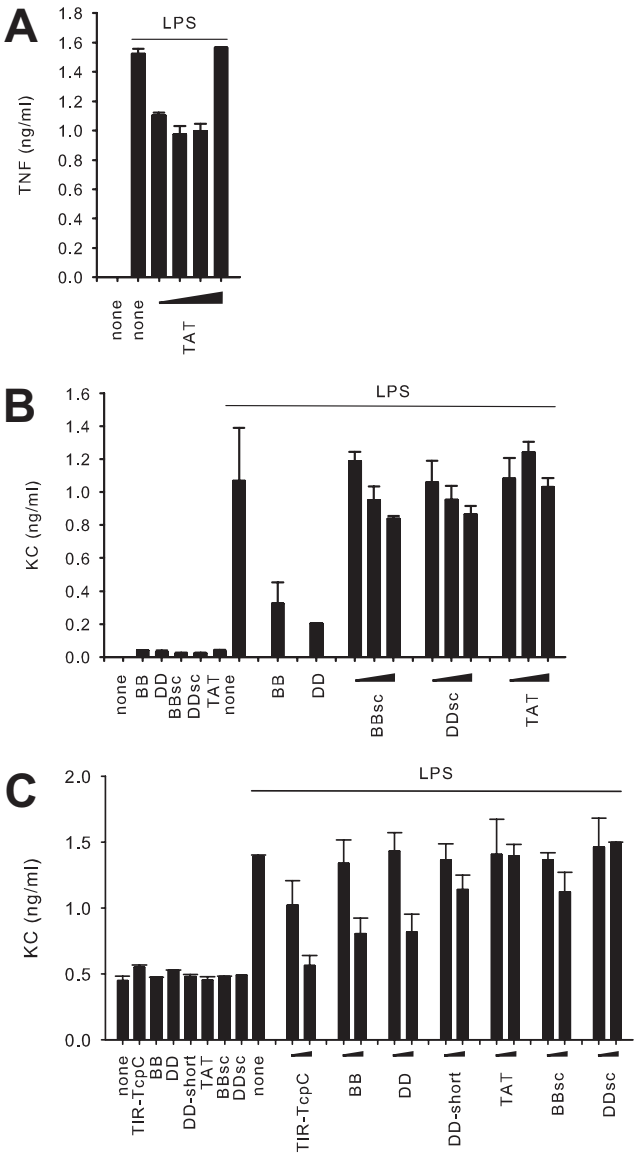

Fig. S5. The BB and DD peptides suppress TLR activation. (*A*) BMDMs were stimulated with ultrapure LPS from *E. coli* (100 ng/mL) in the presence of titrated amounts of the TAT peptide (0.0048, 0.048, 0.48, or 4.8 μM), and the TNF-α in the culture supernatants was analyzed 3 h after stimulation. (*B*) BMDMs were stimulated with LPS as in *A* in the presence of titrated amounts of the TcpC BB peptide (0.026 μM), DD peptide (0.025 μM), scrambled versions of both (BBsc at 0.0026, 0.026, or 0.26 μM and DDsc at 0.0025, 0.025, or 0.25 μM), and the TAT peptide (0.0048, 0.048, or 0.48 μM). The KC content of culture supernatants was analyzed 3 h after stimulation. All peptides at the highest doses were also used in the absence of LPS stimulation. (*C*) Immortalized BMDMs were incubated with titrated amounts of TIR-TcpC (0.006 or 0.06 μM), or BB (0.026 or 0.26 μM), DD (0.025 or 0.25 μM), DD-short (0.033 or 0.33 μM), TAT (0.048 or 0.48 μM), BBsc (0.026 or 0.26 μM), or DDsc (0.025 or 0.25 μM) peptides in the absence or presence of LPS. The KC content of culture supernatants was analyzed 3 h after stimulation. All peptides at the highest doses were also used in the absence of LPS stimulation. Error bars represent SD of three individual experiments.

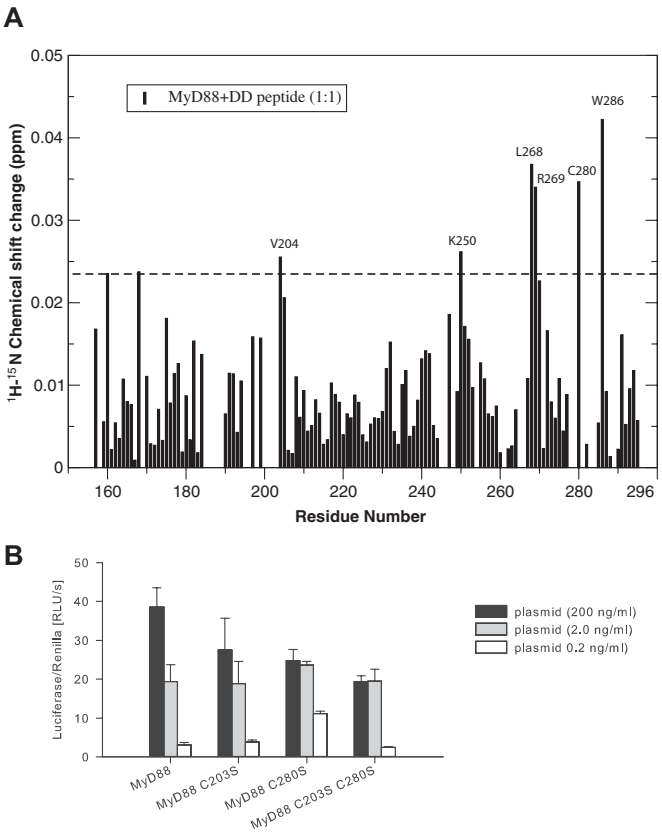

Fig. S6. The MyD88 CD, DE, and EE loops are the primary binding site for the TcpC DD loop. (*A*) Identification of the TcpC "DD-nostrand" peptide binding surface at the MyD88 TIR domain using backbone ^{15}N-^{1}H resonance chemical shift mapping. The interface residues were identified as those with chemical shift changes above the dashed line threshold (mean + 1.5 SD). (*B*) HEK293 cells were transfected with NF-κB firefly luciferase and Renilla luciferase reporter constructs, as well as with titrated amounts of plasmids encoding the wild-type, C203S, C280S, and C203S/C280S mutant MyD88 as indicated. At 48 h after transfection the activity of both luciferases was determined. Error bars represent SD of three individual experiments.

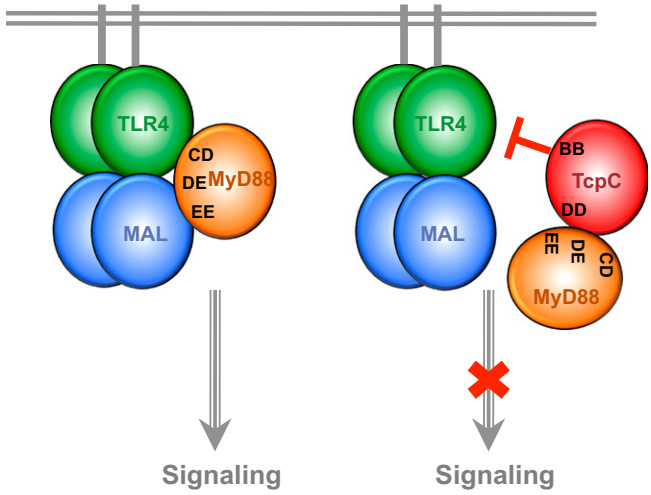

Fig. S7. Model for the TcpC inhibition of the TLR4 signaling complex. The TIR domains are represented as oval spheres for TLR4 (green), MAL (blue), MyD88 (orange), and TcpC (red). The dimerization of the TLR4 TIR domains provides a platform for the MAL TIR domain and MyD88 TIR domain to form a signaling complex, which may involve a surface of the MyD88 TIR domain near its CD, DE, or EE loops (*Left*). In the presence of the TcpC TIR domain (*Right*), MyD88 dissociates from the TLR4:MAL platform and forms a complex with the TcpC TIR domain that is incapable of signaling downstream. This complex of the MyD88 and TcpC TIR domains may involve the DD loop of TcpC and CD, DE, or EE loops of MyD88. The TcpC BB loop may also directly target the TLR4 TIR domain through undefined mechanisms. The depicted monomeric or dimeric forms of the TIR domains are for illustration only, because the exact oligomeric states of the TIR domains during in vivo signaling remain unclear.

Table S1. Crystallographic data collection and refinement

Parameter	Native	Lysine-methylated
Data collection		
Space group	$P2_12_12_1$	$P2_12_12_1$
Resolution (last shell) (Å)	50–1.45 (1.48–1.45)*	50–1.80 (1.91–1.80)*
Unit cell (a, b, c) (Å)	34.9, 56.8, 66.7	33.4, 58.0, 62.5
No. of observations	23051 (947)*	11360 (952)*
Completeness (%)	95.2 (80.3)*	95.9 (81.0)*
*R*merge[†]	0.14 (0.41)*	0.11 (0.47)*
I/σ(I)	30.9 (2.3)*	18 (2.2)*
Redundancy	11.0 (3.7)*	7.9 (4.1)*
Refinement		
No. of protein atoms	1225	1162
No. of hetero-atoms	259	121
rmsd bond lengths (Å)	0.017	0.009
rmsd bond angles (°)	1.073	1.700
Average B-factor (Å^2)	15.7	28.2
Ramachandran plot (favored, allowed, generous, outlier) (%)	99.4, 0.6, 0, 0	95.3, 4.7, 0, 0
*R*work[‡]/*R*free[§] (%)	16.7/19.8 (22.8/30.6)*	18.9/22.8 (22.8/24.1)*
Protein Data Bank code	4EO7	4DOM

*Number corresponding to the last resolution shell.
[†]$R_{merge} = \Sigma_h \Sigma_i |I_i(h) - \langle I(h)\rangle| / \Sigma_h \Sigma_i I_i(h)$, where $I_i(h)$ and $\langle I(h)\rangle$ are the ith and mean measurement of the intensity of reflection *h*.
[‡]$R_{work} = \Sigma_h ||F_{obs}(h)| - |F_{calc}(h)|| / \Sigma_h |F_{obs}(h)|$, where $F_{obs}(h)$ and $F_{calc}(h)$ are the observed and calculated structure factors, respectively. No I/σ cutoff was applied.
[§]R_{free} is the *R* value obtained for a test set of reflections consisting of a randomly selected 5% subset of the data set excluded from refinement.

Table S2. Sequences of the TcpC peptides

Peptide	Sequence
For cell stimulation assay	
BB	NH_2-VIIWYDEQTLEVGDS-Tat-COOH
DD	NH_2-ILPIWHNINAQEVSKY-Tat-COOH
DD-nostrand	NH_2-WHNINAQEVSKY-Tat-COOH
DD-short	NH_2-WHNINAQE-Tat-COOH
BBsc	NH_2-EDYEIISGTVWDQL-Tat-COOH
DDsc	NH_2-HWVNAIISPEQILKYN-Tat-COOH
Tat	NH_2-SAKEIARELAEIAYRRR-COOH
For pull-down assay	
BB-Strep	Acetyl-NH-VIIWYDEQTLEVGDS-ASWSHPQFEK-$CONH_2$
DD-Strep	Acetyl-NH-ILPIWHNINAQEVSKY-ASWSHPQFEK-$CONH_2$